

Modern Physics Letters A
© World Scientific Publishing Company

SOME COMMENTS ON THE HIGH ENERGY EMISSION FROM REGIONS OF STAR FORMATION BEYOND THE GALAXY*

DIEGO F. TORRES[†]

Lawrence Livermore National Laboratory, 7000 East Avenue, L-413, Livermore, CA 94550, USA
dtorres@igpp.ucllnl.org

EVA DOMINGO-SANTAMARIA

Institut de Física d'Altes Energies (IFAE), Edifici C-n, Campus UAB, 08193 Bellaterra, Spain.
domingo@ifae.es

Received (Day Month Year)

Revised (Day Month Year)

Regions that currently are or have been subject to a strong process of star formation are good candidates to be intense γ -ray and neutrino emitters. They may even perhaps be sites where ultra high energy cosmic rays are produced. Outside the Galaxy, the more powerful sites of star formation are found within very active galaxies such as starbursts (SGs) and Luminous or Ultra-Luminous Infrared Galaxies (LIRGs or ULIRGs). Some general characteristic of these objects are herein reviewed from the point of view of their possible status as high energy emitters.

Keywords:

PACS Nos.:

1. Introduction

In this *Brief Review* we discuss some of the recent studies on the high energy emission from regions of star formation located in nearby galaxies, with emphasis on NGC 253.

2. Diffuse γ -ray emission from galaxies

The diffuse γ -ray emission observed from a galaxy basically consists of three components: the truly diffuse emission from the galactic interstellar medium (ISM) itself, the extragalactic background, and the contribution of unresolved faint point-like sources that belong to the galaxy or are beyond it but in the same line-of-sight by

*Solicited review article for Modern Physics Letters A.

[†]Present Address: Instituto de Ciencias del Espacio, Campus UAB, Facultad de Ciencias Torre C-5, pares, 2a planta 08193 Barcelona, Spain

2 *Diego F. Torres & Eva Domingo-Santamaría*

chance. The galactic diffuse emission generated in interactions with the ISM has a wide energy distribution and normally dominates the other components. γ -rays are thus mostly produced in energetic interactions of particles with the interstellar gas and the radiation fields present in the galaxy. The diffuse γ -ray emission at high energies mainly comes from the interaction of high energy cosmic ray nucleons with gas nuclei via neutral pion production. Contributions from energetic cosmic ray electrons interacting with the existing photon fields via inverse Compton scattering and with the matter field of the galaxy via relativistic bremsstrahlung are generally more important below 100 MeV. Since these processes are dominant in different parts of the energy domain, information about the overall spectrum of the cosmic ray population can be extracted.

If γ -rays absorption in the galaxy is neglected, the diffuse γ -ray flux can be estimated as the line-of-sight integral over the emissivity of the ISM. The latter is essentially the product of the cosmic ray spectrum, the density of the gas or radiation field in the galaxy, and the corresponding cross section for a given process. Therefore, γ -ray measurements together with estimations of the gas content and photon field densities provide a tool to determine the cosmic rays spectrum. The interstellar hydrogen distribution (in its molecular form, H_2 , atomic, HI, or ionized, HII) is derived from radio surveys. It can be traced from the emission lines of molecules that get radiatively or collisionally excited, by means of corresponding calibrations or conversion factors. CO molecules are generally the primary tracers of molecular hydrogen (e.g., Dame et al. 2001). CO is a polar molecule with strong dipole rotational emission at millimeter-wavelengths. H_2 , though much more abundant than CO, has only a weak quadrupole signature. Generally, the conversion factor between CO luminosity and molecular mass is estimated and constrained from measurements in our own Galaxy where masses of individual molecular clouds can be independently determined from cloud dynamics (e.g., Solomon et al. 1987; Young & Scoville 1991). Alternatively, assuming the spectrum of cosmic rays of the Galaxy and a given γ -ray flux, it is possible to obtain a calibration for the CO luminosity to estimate the conversion factor (e.g., Bloemen et al. 1986). The atomic neutral hydrogen content can be estimated through the intensity of 21-cm emission line. HCN, CS and HCO^+ are the most frequently observed interstellar molecules after CO. Due to their higher dipole moment they require about two orders of magnitude higher gas densities for collisional excitation than CO. HCN is one of the most abundant high dipole moment molecules and traces molecular gas at densities $n(H_2) \gtrsim 3 \times 10^4 \text{ cm}^{-3}$, compared to densities of about $\gtrsim 500 \text{ cm}^{-3}$ traced by CO. Because of this fact, dense regions associated with star formation sites are usually better traced at the higher HCN frequencies.

2.1. *Diffuse γ -ray emission from the Galaxy*

Studies of the Galactic diffuse γ -ray emission provide privileged insights into the generation processes of γ -rays in galactic environments. The diffuse γ -ray continuum

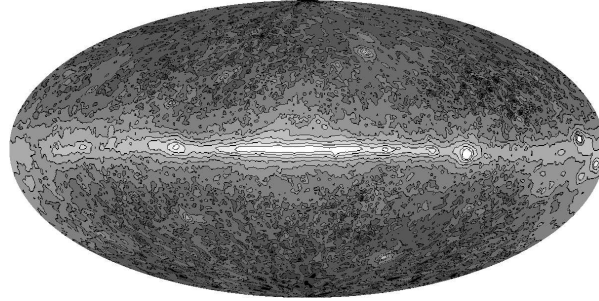


Fig. 1. Intensity of γ -rays (> 100 MeV) observed by EGRET. The broad, intense band near the equator is interstellar diffuse emission from the Milky Way. The intensity scale ranges from $1 \times 10^{-5} \text{ cm}^{-2} \text{ s}^{-1} \text{ sr}^{-1}$ to $5 \times 10^{-4} \text{ cm}^{-2} \text{ s}^{-1} \text{ sr}^{-1}$ in ten logarithmic steps. The data is slightly smoothed by convolution with a gaussian of FWHM 1.5° . Courtesy: EGRET Collaboration.

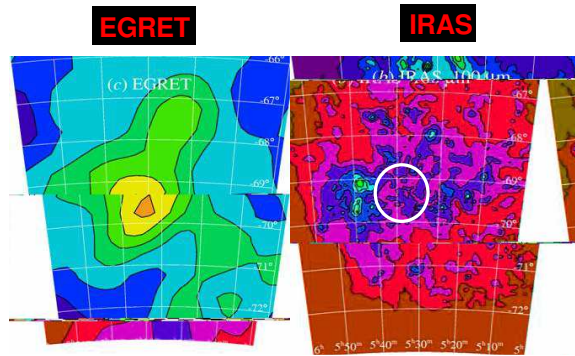


Fig. 2. LMC as seen by EGRET (γ -rays) and IRAS (infrared). White circle indicates the position of 30 Doradus, a large molecular cloud and intense star formation region. Courtesy: Seth Digel.

emission is in fact the dominant feature of the γ -ray sky of the Milky Way (see the EGRET γ -ray map above 100 MeV presented in Figure 1), approximately amounting 90% of the high energy γ -ray luminosity ($\sim 1.3 \times 10^6 L_\odot$, Strong, Moskalenko, & Reimer 2000). This emission, in the range of 50 KeV to 50 GeV, was systematically studied by all the past hard X-ray/ γ -ray satellites, from SAS-2 and COS-B in the 70's and early 80's, to the OSSE, COMPTEL and EGRET experiments onboard of the Compton Gamma-Ray Observatory (CGRO), launched in 1990, as well as, more recently, by INTEGRAL (Lebrun et al. 2004). Hunter et al. (1997) present a review of CGRO observations.

2.2. Detection (and non-detection) of other local group galaxies

To date, the Large Magellanic Cloud (LMC) is the only external galaxy that has been detected in the light of its diffuse γ -ray emission (Sreekumar et al. 1992). This fact is explained by the isotropic flux dilution by distance. At 1 Mpc, for example,

4 *Diego F. Torres & Eva Domingo-Santamaría*

the flux of the Milky Way would approximately be 2.5×10^{-8} photons $\text{cm}^{-2} \text{s}^{-1}$ above 100 MeV, well below the sensitivity achieved up to now by the γ -ray missions in the relevant energy domain. Although normal galaxies, or even galaxies with fairly intense star formation such as the LMC, are quite numerous, their distances ought to make them very faint γ -ray sources.

The LMC was detected by EGRET with a flux of $(1.9 \pm 0.4) \times 10^{-7}$ photons $\text{cm}^{-2} \text{s}^{-1}$ above 100 MeV (see Figure 2). Interestingly, as can be noticed in Figure 2, the distribution of the diffuse γ -ray emission from the LMC is consistent with the infrared IRAS map profile, being the more intense γ -ray emission region in spatial coincidence with the position of 30 Doradus, a particular region of the LMC with large molecular clouds and extensive ongoing star formation. This correspondence is indeed the reason why the EGRET team claimed the detection of the LMC. This result had been predicted by Fichtel et al. (1991) as the output of pion decay resulting from the interaction between cosmic ray protons and interstellar gas, assuming galactic dynamic balance between the expansive pressures of the cosmic rays, magnetic fields and kinematic motions, and the gravitational attraction of matter.

It is instructive to show how to obtain the predicted flux and what consequences it has in our understanding of cosmic ray generation. One can consider that the electron spectrum is a power-law $N(E)dE = KE^{-\gamma}dE$, with $N(E)$ being the number of electrons per unit energy per unit volume, and K the spectrum normalization. The intensity of the synchrotron radiation in the presence of random magnetic fields is

$$I_\nu = 1.35 \times 10^{-22} a(\gamma) L K B^{(\gamma+1)/2} \left(\frac{6.26 \times 10^{18}}{\nu} \right)^{(\gamma-1)/2} \text{ erg cm}^{-2} \text{ s}^{-1} \text{ sr}^{-1} \text{ Hz}^{-1}, \quad (1)$$

(Ginzburg & Syrovatskii 1964) where ν is the observing radio frequency in Hz, $a(\gamma)$ is a numerical coefficient of order 0.1, L is the length over which the electrons and magnetic fields are present and B is the magnetic field strength. The normalization of the spectrum is assumed proportional to B^2 both in the LMC and our Galaxy, and the shape of the spectrum in the LMC is assumed the same as that in the Milky Way. Then, if K_0 and B_0 are the corresponding values of these parameters in our Galaxy, and $w(x)K_0$ is the value in the LMC, $B = w(x)^{1/2}B_0$. Using this expression in Eq. (1) the scaling can be determined as

$$w(x) = \left(\frac{2.40I_\nu}{a(\gamma)L_{21}K_0} \right)^{4/\gamma+5} B_0^{-2(\gamma+1)/(\gamma+5)} \left(\frac{\nu}{6.26 \times 10^{18}} \right)^{2(\gamma+1)/(\gamma+5)}, \quad (2)$$

where $L_{21} = L/(3.09 \times 10^{21} \text{cm})$ is the distance in kpc. Assuming best guesses for all parameters involved (see, for instance, the Appendix of Fichtel et al. 1991), the electron normalization can be determined. The additional assumption that the electron-to-proton ratio is the same in the LMC as in the Galaxy yields the proton spectrum. An estimation of the matter column density then allows the γ -ray flux

to be computed as:

$$F(E > 100\text{MeV}) \simeq \int d\Omega \left[2 \times 10^{-25} \times \frac{w(x)}{4\pi} \times \int dl(n_a + n_m) \right] \frac{1}{4\pi d^2} \text{photons s}^{-1} \text{cm}^{-2} \quad (3)$$

with $d\Omega$ being the solid angle subtended by the emitting region, $j_\gamma = 2 \times 10^{-25} \times w(x)/4\pi$ photons $\text{s}^{-1} \text{sr}^{-1} \text{H-atom}^{-1}$ being the γ -ray production, and $\int dl(n_a + n_m)$, with n_a and n_m the atomic and molecular density, respectively, being the column density. Note that the prediction allows different emission level contours to be plotted, depending on the position in the galaxy. However, in order to make a direct comparison with EGRET or any other experiment, the predicted γ -ray intensity has to be compared with the corresponding point-spread function. Although the predicted intensity based on the dynamic balance is in good agreement with the EGRET result, it is also in agreement with the cosmic ray density being the same throughout the galaxy, as if, for instance, the cosmic ray density were universal in origin (as proposed, for instance, by Brecher and Burbidge 1972).

The Small Magellanic Cloud (SMC) was also observed by EGRET, but no detection was found. An upper limit of 0.5×10^{-7} photons $\text{cm}^{-2} \text{s}^{-1}$ was set for the γ -ray emission above 100 MeV (Sreekumar et al. 1993). If the cosmic ray density in the SMC were as high as it is in our Galaxy, the flux in γ -rays would be $\sim 2.4 \times 10^{-7}$ photons $\text{cm}^{-2} \text{s}^{-1}$, a level incompatible with the experimental result. It was then the non-detection of the SMC what defined that the distribution of cosmic rays is galactic in origin, local to accelerators and thus enhanced in regions of star formation rather than universal.

Very recently, Pavlidou and Fields (2001) presented an observability study for several of the local group galaxies, assuming that the γ -ray flux above 100 MeV is represented by

$$F(E > 100\text{MeV}) = 2.3 \times 10^{-8} f_G \left(\frac{\Sigma}{10^4 \text{M}_\odot \text{kpc}^{-2}} \right) \text{photons cm}^{-2} \text{s}^{-1}, \quad (4)$$

with f_g being the ratio between the galaxy G and the Milky Way supernova rates, and Σ the gas mass-to-distance squared ratio. This amounts to the assumption that supernova remnants alone are the source of cosmic rays, and that once produced, their propagation is described by a leaky box model, with the additional supposition of an equal time/length of escape to that of our Galaxy. This approach is far simpler than that followed by Fichtel, Sreekumar and coworkers when analyzing the LMC and SMC cases, and probably not quite correct, especially for those galaxies which are different from ours, like the SMC. For example, the Andromeda galaxy M31, a case studied previously by Özel and Berkhuijsen (1987), would present a flux of 1×10^{-8} photons $\text{cm}^{-2} \text{s}^{-1}$, consistent with the observational upper limit set by Blom et al. (1999) using more recent EGRET data. This flux could be detected by GLAST in the first 2 years of its all-sky survey with 14σ significance. If such is the case, it will be possible to study the correlation between regions of higher column

density and higher γ -ray emission. It could even be possible to observe effects of the magnetic torus (e.g., Beck et al. 1996) and the star forming ring (e.g., Pagani et al. 1999), a morphological feature analogous to the Milky Way's H_2 ring extending in radius from 4 to 8 kpc (e.g., Bronfman et al. 1988), which has been detected in γ -ray surveys (Stecker et al. 1975). Other results for Local Group Galaxies show that, unless the assumptions are severely misrepresenting the physics, only M33 might have some chance of being detected by future instruments (Digel et al. 2000).

3. Galaxies with higher star formation rate

Galaxies where star formation is a powerful active process may be able to compensate the dilution effect produced by their distance to Earth. The large masses of dense interstellar gas and the enhanced densities of supernova remnants and massive young stars expected to be present in such galaxies suggest that they emit γ -ray luminosities orders of magnitude greater than normal galaxies. Such environments will typically emit a large amount of infrared (IR) radiation, because abundant dust molecules absorb the UV photons emitted by the numerous young massive stars and reemit them as IR radiation. Therefore, the infrared luminosity, L_{IR} , of a galaxy can (but not always) be an indication of star formation taking place in it.

Luminous infrared galaxies (LIRGs) have been identified as a class, generally selected for emitting more energy in the IR band ($\sim 50 - 500 \mu\text{m}$) than in all other wavelengths combined. The most luminous galaxies in the IR band constitute by themselves a subclass of the more powerful galaxies ever known. LIRGs are defined as galaxies with IR luminosities larger than $10^{11} L_{\odot}$. Those with $L_{\text{IR}} > 10^{12} L_{\odot}$ are called ultraluminous infrared galaxies (ULIRGs). See Sanders & Mirabel (1996) for an extensive review about these objects. LIRGs are the dominant population of extragalactic objects in the local universe ($z < 0.3$) at bolometric luminosities above $L > 10^{11} L_{\odot}$, ULIRGs are in fact the most luminous local objects. Our current understanding of LIRGs and ULIRGs suggests that they are recent galaxy mergers in which much of the gas of the colliding objects, particularly that located at distances less than ~ 5 kpc from each of the pre-merger nuclei, has fallen into a common center (typically less than 1 kpc in extent), triggering a huge starburst (e.g., Sanders et al. 1988, Melnick & Mirabel 1990). The size of the inner regions of ULIRGs, where most of the gas is found, can be even as small as a few hundreds parsecs; there, a large nuclear concentration of molecular gas is found. Supporting the idea that IR luminosities in LIRGs are mainly due to starburst regions rather than to enshrouded AGNs it is the fact that LIRGs not only possess a large amount of molecular gas, but a large fraction of it is at high density (e.g., Gao & Solomon 2003a, 2003b). This makes them prone to star formation, and thus to have significant CR enhancements. In addition, there is evidence for the existence of extreme starburst regions within LIRGs (see, e.g., Downes & Solomon 1998). These, larger than giant molecular clouds but with densities found only in small cloud cores, appear to be the most outstanding star-forming regions in the local universe (each

representing about 1000 times as many OB stars as 30 Doradus). They are well traced by HCN emission, i.e., they represent a substantial fraction of the whole HCN emission observed for the whole galaxy (Downes & Solomon 1998, Solomon et al. 1992). The CR enhancement factor in these small but massive regions can well exceed the average value for the galaxy.

To date, no LIRGs or ULIRGs, nor any other starburst galaxy has been detected in γ -rays by EGRET, upper limits were imposed for M82, $F(E > 100\text{MeV}) < 4.4 \times 10^{-8}$ photons $\text{cm}^{-2} \text{s}^{-1}$, and NGC 253, $F(E > 100\text{MeV}) < 3.4 \times 10^{-8}$ photons $\text{cm}^{-2} \text{s}^{-1}$ (Blom et al. 1999), the two nearest starbursts. Similar constraints were found for many LIRGs by means of a search in existing EGRET data for the fluxes of likely γ -ray-bright LIRGs (Torres et. al. 2004, Cillis et al. 2005).

3.1. Should we detect them?

Neglecting possible CR density gradients within the interstellar medium of the galaxy, the hadronically-generated γ -ray number luminosity (photons per unit of time) is given by:

$$I_\gamma(E_\gamma) = \int n(r)q_\gamma(E_\gamma)dV = \frac{M}{m_p}q_\gamma, \quad (5)$$

where r represents the position within the interaction region V , M is the mass of gas, m_p is the proton mass, n is the number density, and q_γ is the γ -ray emissivity (photons per unit of time per atom). The γ -ray flux is then:

$$F(> 100 \text{ MeV}) = \frac{I_\gamma(> 100 \text{ MeV})}{4\pi D_L^2}, \quad (6)$$

where D_L is the luminosity distance in a Friedman universe.^a In an appropriate scaling, the γ -ray flux can be estimated from:

$$F(> 100 \text{ MeV}) \sim 2.4 \times 10^{-9} \left(\frac{M}{10^9 M_\odot} \right) \left(\frac{D_L}{\text{Mpc}} \right)^{-2} k \text{ photons cm}^{-2}\text{s}^{-1}. \quad (8)$$

The previous estimation introduces k as the enhancement factor of γ -ray emissivity in the galaxy under study compared to the local value near the Earth. If the slope

^aThe luminosity distance describes the distance at which an astronomical body would lie based on its observed luminosity. If a source of luminosity L emits into a non-expanding universe, the integral of the photon flux over a sphere of given radius will be equal to the source luminosity. In an expanding space-time, the photon wavelength is redshifted, diluting the energy over the sphere by a factor of $(1+z)$, where z is the redshift. Another factor $(1+z)$ is introduced as the emission rate of the photons from the source is time dilated with respect to an observer due to the Doppler effect. Therefore, the observed luminosity is attenuated by two factors: relativistic redshift and the Doppler shift of emission, each of them contributing a $(1+z)$ attenuation. The luminosity distance can be expressed in terms of the Hubble parameter, H_0 , the deceleration parameter, q_0 , and the redshift:

$$D_L = \frac{c}{H_0 q_0^2} \left[1 - q_0 + q_0 z + (q_0 - 1) \sqrt{2q_0 z + 1} \right]. \quad (7)$$

8 *Diego F. Torres & Eva Domingo-Santamaría*

of the CR spectrum at the galaxy does not differ much from that existing near the Earth, what clearly is a rough approximation, k can be at the same time an estimator of the enhancement of CR energy density: $k \equiv q_\gamma/q_{\gamma,\oplus} \sim \omega/\omega_\oplus$, with $q_{\gamma,\oplus} = 2.4 \times 10^{-25}$ photons s^{-1} H-atom $^{-1}$ being the γ -ray emissivity of the interstellar medium at the Earth neighborhood, and ω_\oplus being the CR energy density near Earth. The numerical factor of Equation (8) already takes into account the γ -ray emissivity from electron bremsstrahlung (see, e.g., Pavlidou & Fields 2001 and references therein).^b Note that $F(> 100 \text{ MeV}) \sim 2.4 \times 10^{-9}$ photons $\text{cm}^{-2}\text{s}^{-1}$ is approximately the GLAST satellite sensitivity after 1 yr of all-sky survey. Therefore, from Equation (8), having an estimation of the mass gas content of the galaxy through the measured CO luminosity, the minimum average value of k for which the γ -ray flux above 100 MeV will be at least 2.4×10^{-9} photons $\text{cm}^{-2} \text{s}^{-1}$ can be computed:

$$\langle k \rangle_{min} = \left(\frac{M_{H_2}}{10^9 M_\odot} \right)^{-1} \left(\frac{D_L}{\text{Mpc}} \right)^2. \quad (9)$$

This approach represents a first step in order to establish the plausibility of the future detection of a given LIRG or SG in the γ -ray band. A similar estimation can be made for the TeV flux expected from these objects. Völk et al. (1996) found:

$$F(> 1 \text{ TeV}) \sim 1.7 \times 10^{-13} \left(\frac{E}{\text{TeV}} \right)^{-1.1} \left(\frac{M}{10^9 M_\odot} \right) \left(\frac{D_L}{\text{Mpc}} \right)^{-2} k \text{ photons cm}^{-2}\text{s}^{-1}, \quad (10)$$

where a power law slope of 2.1 is assumed for the CR spectrum. For comparison, it is useful to keep in mind that an integrated flux above 1 TeV of about 1×10^{-13} photons $\text{cm}^{-2} \text{s}^{-1}$ is the expected 5σ flux sensitivity for a 50 hr observation at small zenith angle of the new ground-based imaging atmospheric Čerenkov telescopes (IACTs). Then, those galaxies that might appear in the new GeV catalogs might also constitute new targets for the ground-based telescopes at higher energies, provided their proton spectrum are sufficiently hard.^c

However, obtaining reasonable values for the minimum $\langle k \rangle$ required for detection is not a sufficient condition to claim the plausibility for a galaxy to be a gamma-ray source: it is also needed that the particular galactic environment is active enough as to provide the minimum computed $\langle k \rangle$ value. A first indication of the average value of the CR enhancement in a given galaxy can be indirectly estimated from the star

^bNote that γ -rays can also be produced by inverse Compton interactions with the strong FIR field of the galaxy. However, this contribution has been disregarded in favor of the hadronic channel (between accelerated protons and diffuse material of density n), which is a well justified approach above 100 MeV (see below). We also disregard additional hadronic production of high energy γ -rays with matter in the winds of stars (see e.g. Romero & Torres 2003, Torres et al. 2004b).

^cIn addition, the signal-to-noise ratio in neutrino telescopes (neutrinos will be unavoidably produced in hadronic interactions leading to charged pions) can be approximately computed starting from the γ -ray flux (see, e.g., Anchordoqui et al. 2003b). LIRGs could be new candidate sources for ICECUBE if they are detectable sources of TeV photons.

formation rate (SFR), quantity that can be directly related to observations. More star formation implies a higher supernova explosion rate, and as this happens, there are more cosmic ray acceleration sites and thus an enhanced cosmic ray density. Therefore, a reasonable first assumption is (e.g., Drury et al. 1994, Aharonian & Atoyan 1996, Torres et al. 2003, etc.):

$$\langle k \rangle \equiv \frac{q_\gamma}{q_{\gamma,\oplus}} \sim \frac{\omega_{CR}}{\omega_{CR,\oplus}} \sim \frac{SNrate}{SNrate_{MW}} \sim \frac{SFR}{SFR_{MW}}. \quad (11)$$

The SFR is highly correlated to the quantity of dense molecular gas present in the galaxy, as can be seen in Gao and Solomon (2003b) figure 6,

$$SFR = 1.8 \left(\frac{M_{dense}}{10^8 M_\odot} \right) \left(\frac{10}{\alpha_{HCN}} \right) M_\odot \text{yr}^{-1}. \quad (12)$$

The dense mass is traced by the HCN emission and it is found to be proportional to the HCN luminosity (Gao and Solomon 2003a):

$$M_{dense} = \alpha_{HCN} L_{HCN} \sim 10 \left(\frac{L_{HCN}}{\text{K km s}^{-1} \text{pc}^2} \right) M_\odot. \quad (13)$$

Therefore:

$$SFR = 18 \left(\frac{L_{HCN}}{10^8 \text{K km s}^{-1} \text{pc}^2} \right) M_\odot \text{yr}^{-1}. \quad (14)$$

The Milky Way star formation rate (quoted as SFR_\oplus) can be also estimated from Equation (14), being the HCN luminosity $L_{HCN}(MW) \sim 0.04 \times 10^8 \text{K km s}^{-1} \text{pc}^2$ (e.g., Solomon et al. 1992, Wild & Eckart 2000). Then, a plausible value of the CR enhancement (obtained as the ratio between the SFR of the galaxy and that of our Milky Way) can be computed for each HCN galaxy. Figure 3 shows these values versus the needed k in order to make the galaxy detectable by GLAST/LAT. Only galaxies appearing above or around the line of unit slope can be considered prime candidates for detection. While a galaxy with high L_{HCN}/L_{CO} ratio (i.e., with a high mass fraction of dense gas) will be a LIRG (or a ULIRG), the converse is not always true (Gao & Solomon 2003a). There are gas-rich galaxies which are LIRGs only because of the huge amount of molecular gas they possess, not because they have most of it at high density (and thus are undergoing a particularly strong starburst phenomenon). In some of these cases, while the value of enhancement needed for detection might only be of a few hundreds, the plausible value of k is much lower, since no strong star formation is ongoing (e.g., NGC 1144, Mrk 1027, NGC 6701, and Arp 55, which appear to be using the huge molecular mass they have in creating stars at a normal SFR). In the context of γ -ray observability, GLAST will detect those galaxies that, being close enough, not only shine in the FIR but that do so *because* of their active strong star formation processes.

logic of the code is shown schematically in Figure 4. As starting point, an injection spectrum of primary cosmic rays is assumed. Its characteristics are estimated by linking the cosmic rays to the known (local to the source) acceleration processes that may have created them (e.g., supernova remnants induced shocks or collective effects of stellar winds), and thus using the related observational inputs, as the supernova explosion rate. The primary proton population is subject to energy losses (by ionization and pion production) and to escaping out from the emission region through diffusion or convection processes. From the proton steady state (i.e. the solution of the diffusion-loss equation), the computation of the secondaries is done. Secondary electrons and positrons are generated from knock-on interactions and decay of secondary charged pions. The contribution of secondary electrons and positrons is then summed up to the primary electron population, which is generally assumed to be the same than the proton injection spectrum but by a factor N_e/N_p . The whole electron/positron population is then let to evolve to its steady state, computing the energy losses that it is subject to (synchrotron emission, ionization, bremsstrahlung, inverse Compton, and adiabatic losses) and the confinement timescale. The radio spectrum is then evaluated from the steady electrons synchrotron emission, modulated by free-free absorption of the medium plasma electrons. A comparison between the predicted radio flux and the existing data provides a direct feedback to some model parameters that appear in the computation of the electron steady state. They are tuned until a good agreement with the measured radio spectrum is achieved. For example, one of the crucial parameters, which indeed is hardly known with good precision in most of the scenarios but plays an important role both in the electron synchrotron energy losses and in the synchrotron radio emission, is the magnetic field. Other parameter crucial in explaining low frequency radio data is the absorption frequency of free-free radiation (alternatively, the emission measure and plasma temperature). These two, are determined within the code until an agreement with observations is reached. Infrared emission from dust existing in the region is also simulated with the parameters that characterize the infrared photon field being adjusted to describe the observational existing data. These photons are the seed of inverse Compton process, either when considering the electron energy losses or the resultant high energy γ -ray emission. Once all the parameters have been fixed and the proton and electron steady populations have been determined, high energy γ -ray emission is evaluated. This includes the decay of neutral pions, and leptonically-generated γ -rays, through bremsstrahlung and inverse Compton of the steady electron population. Photon absorption through gamma-gamma and gamma-Z processes are considered to obtain the final predictions of fluxes.

5. Example: the case of NGC 253

5.1. Phenomenology of the central region of NGC 253

NGC 253 is located at a distance of ~ 2.5 Mpc and it is a nearly edge-on (inclination 78°) barred Sc galaxy. The continuum spectrum of NGC 253 has a luminosity of

$4 \times 10^{10} L_{\odot}$ (Melo et al. 2002). The FIR luminosity is at least a factor of 2 larger than that of our own Galaxy, and it mainly comes from the central nucleus. IR emission can be understood as cold ($T \sim 50K$) dust reprocessing of stellar photon fields.

When observed at 1 pc resolution, at least 64 individual compact radio sources have been detected within the central 200 pc of the galaxy (Ulvestad & Antonucci 1997), and roughly 15 of them are within the central arcsec of the strongest radio source, considered to be either a buried active nucleus or a very compact SNR. Of the strongest 17 sources, about half have flat spectra and half have steep spectra. This indicates that perhaps half of the individual radio sources are dominated by thermal emission from H II regions, and half are optically thin synchrotron sources, presumably SNRs. There is no compelling evidence for any sort of variability in any of the compact sources over an 8 yr time baseline. The region surrounding the central 200 pc has also been observed with subarcsec resolution and 22 additional radio sources stronger than 0.4 mJy were detected within 2kpc of the galaxy nucleus (Ulvestad 2000). The region outside the central starburst may account for about 20% of the star formation of NGC 253. It is subject to a supernova explosion rate well below 0.1 yr^{-1} , and has an average gas density in the range $20\text{--}200 \text{ cm}^{-3}$, much less than the most active nuclear region (Ulvestad 2000).

Carilli (1996) presented low frequency radio continuum observations of the nucleus at high spatial resolution. Free-free absorption was claimed to be the mechanism producing a flattening of the synchrotron curve at low energies, with a turnover frequency located between $10^{8.5}$ and 10^9 Hz. The emission measures needed for this turnover to happen, for temperatures in the order of 10^4 K, is at least 10^5 pc cm^{-6} . As shown by infrared, millimeter, and centimeter observations, the 200 pc central region dominates the current star formation in NGC 253, and is considered as the starburst central nucleus (e.g., Ulvestad and Antonucci 1997, Ulvestad 2000). Centimeter imaging of this inner starburst, and the limits on variability of radio sources, indicates a supernova rate less than 0.3 yr^{-1} (Ulvestad & Antonucci 1997), which is consistent with results ranging from 0.1 to 0.3 yr^{-1} inferred from models of the infrared emission of the entire galaxy (Rieke et al. 1980; Rieke, Lebofsky & Walker 1988, Forbes et al. 1993). When compared with Local Group Galaxies, the supernova rate in NGC 253 is one order of magnitude larger (Pavlidou and Fields 2001).

Current estimates of the gas mass in the central $20'' - 50''$ (< 600 pc) region range from $2.5 \times 10^7 M_{\odot}$ (Harrison, Henkel & Russell 1999) to $4.8 \times 10^8 M_{\odot}$ (Houghton et al. 1997), see Bradford et al. (2003), Sorai et al. (2000), and Engelbracht et al. (1998) for discussions. For example, using the standard CO to gas mass conversion, the central molecular mass was estimated as $1.8 \times 10^8 M_{\odot}$ (Mauersberger et al. 1996). It would be factor of ~ 3 lower if such is the correction to the conversion factor in starburst regions which are better described as a filled intercloud medium, as in the case of ULIRGs, instead of a collection of separate large

molecular clouds, see Solomon et al. (1997), Downes & Solomon (1998), and Bryant & Scoville (1999) for discussions. Thus we will assume in agreement with the mentioned measurements that within the central 200 pc, a disk of 70 pc height has $\sim 2 \times 10^7 M_{\odot}$ uniformly distributed, with a density of $\sim 600 \text{ cm}^{-3}$. Additional target gas mass with an average density of $\sim 50 \text{ cm}^{-3}$ is assumed to populate the central kpc outside the innermost region, but subject to a smaller supernova explosion rate $\sim 0.01 \text{ yr}^{-1}$, 10% of that found in the most powerful nucleus (Ulvestad 2000).

5.2. The multi-frequency emission from NGC 253

The numerical solution of the diffusion-loss equation for protons and electrons in NGC 253 is shown in Figure 5a and 5b for an adopted diffusive residence timescale of 10 Myr, a convective timescale of 1 Myr, and a density of $\sim 600 \text{ cm}^{-3}$. In the case of electrons, the magnetic field with which synchrotron losses are computed in Figure 5b is $300 \mu\text{G}$. The latter is fixed requiring that the steady electron population produces a flux level of radio emission matching observations. An injection electron spectrum is considered –in addition to the secondaries– in generating the steady electron distribution. From about $E_e - m_e \sim 10^{-1}$ to 10 GeV, the secondary population of electrons dominates, in any case. The IR continuum emission is modelled with a spectrum having a dilute blackbody (graybody) emissivity law, proportional to $\nu^{\sigma} B(\epsilon, T)$, where B is the Planck function. Figure 1c shows the result of this modelling and its agreement with observational data when the dust emissivity index $\sigma = 1.5$ and the dust temperature $T_{\text{dust}} = 50\text{K}$. Whereas free-free emission is subdominant when compared with the synchrotron flux density, free-free absorption plays a key role at low frequencies, determining the opacity. We have found a reasonable agreement (see Figure 1d) with all observational data for a magnetic field in the innermost region of $300 \mu\text{G}$, an ionized gas temperature of about 10^4 K, and an emission measure of $5 \times 10^5 \text{ pc cm}^{-6}$. Figure 1e shows bremsstrahlung, inverse Compton, and pion decay γ -ray fluxes from the central nucleus of NGC 253. These results are obtained with the model in agreement with radio and IR observations. These predictions, while complying with EGRET upper limits, are barely below them. If this model is correct, NGC 253 is bound to be a bright γ -ray source for GLAST. The integral fluxes are shown in Figure 1f. This model predicts that, given enough observation time, NGC 253 is also to appear as a point-like source in an instrument like HESS. The HESS array presented results for NGC 253, based on a total of 28 hours taken during the construction of the array with 2 telescopes operating (Aharonian et al. 2005). The energy threshold for this dataset was 190 GeV. Upper limits from HESS on the integral (99 % confidence level) are shown in Figure 1f. As an example, above 300 GeV, the upper limit is $1.9 \times 10^{-12} \text{ photons cm}^{-2} \text{ s}^{-1}$. The predictions for NGC 253 are below these upper limits at all energies but still above HESS sensitivity for reasonable observation times. The effect of the opacity on the integral γ -ray fluxes only plays a role above 3 TeV.

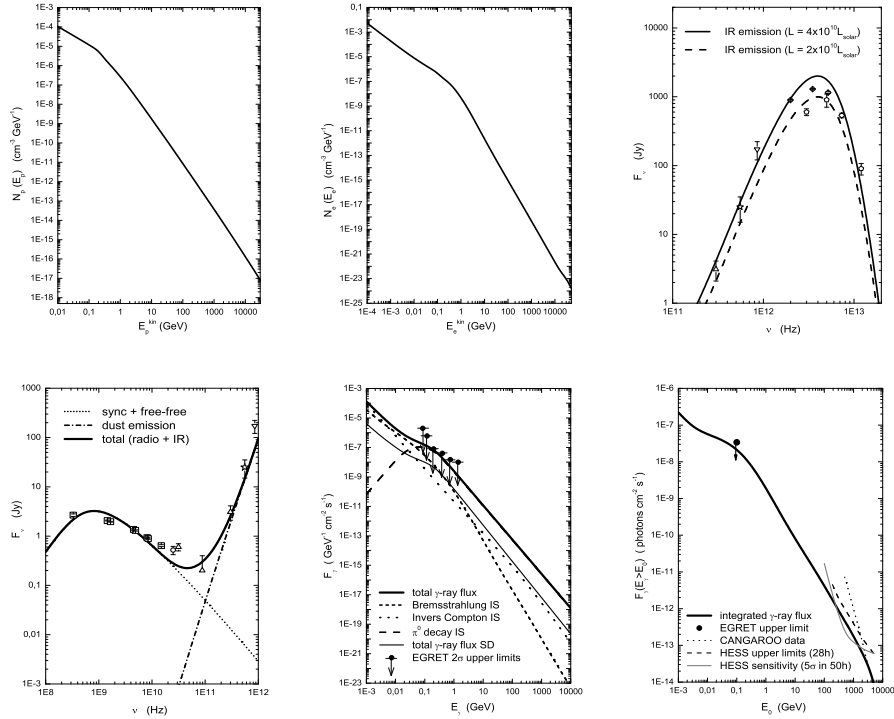


Fig. 5. From top to bottom and left to right: a) Steady proton distributions in the innermost region of NGC 253. b) Idem for the steady electron distribution. c) IR flux from NGC 253 assuming a dilute blackbody with temperature $T_{\text{dust}} = 50$ K and different total luminosities. d) Multifrequency spectrum of NGC 253 from radio to IR and comparison with experimental data points. e) Differential γ -ray fluxes from the central region of NGC 253. Total contribution of the surrounding disk is separately shown, as are the EGRET upper limits. Also shown are the relative contributions of bremsstrahlung, inverse Compton, and neutral pion decay to the γ -ray flux. f) Integral γ -ray fluxes. The EGRET upper limit (for energies above 100 MeV), the CANGAROO (Itoh et al. 2002) integral flux as estimated from their fit, the (4 telescopes) HESS sensitivity (for a 5σ detection in 50 hours), and the (2 telescopes) HESS upper limit curve on NGC 253 (Aharonian et al. 2005) are given. Absorption effects are already taken into account. From Domingo-Santamaría and Torres (2005).

6. Predictions at the highest energies and differential cross section parameterization: application to Arp 220

Numerical calculations of the γ -ray flux produced through π^0 decay involve the differential cross-section of proton-proton (pp) interactions, for which experimental data to confront with only exists up to the GeV range. Therefore, extrapolation of the differential pp cross section to higher energies (as needed in the kind of scenarios herein discussed) induces large uncertainties in the resultant γ -ray flux. An analysis of the effect of the currently available differential cross section parameterizations over the high energy γ -ray flux can be found in the appendix of Domingo-Santamaría

and Torres (2005). For γ -rays above few TeV (i.e., γ -rays mostly generated by protons above few tens of TeV), the Blattnig et al. (2000) differential cross section parameterization makes the γ -ray emitted spectrum much harder than the proton spectrum that produced them. This indicates that a direct extrapolation of Blattnig et al. parameterization above TeV induces significant overpredictions of fluxes.

Consider Arp 220, for which there is a multiwavelength model already presented in the literature (Torres 2004).^d At the time this modelling was made, it was unclear whether the Blattnig et al. (2000) parameterization (which actually produces the right total cross section at all energies) would also produce the correct differential cross section above 100 GeV, and it was then incorporated into the `Q-DIFFUSE` code to compute the neutral pion γ -ray production. As discussed, this yield to overestimates of fluxes above 100 GeV, where Blattnig et al. parameterization should not be used. New estimates of the neutral pion decay contribution to the γ -ray flux expected from Arp 220 have been calculated for this paper using more reliable approaches to the cross section at high energies, and are shown in Figure 6, see Domingo-Santamaría and Torres (2005) for a discussion on the parameterizations used. This comparison uses the same galactic model in every other respect, but just different differential cross sections.

Although the prediction of a possible detection of Arp 220 by the GLAST satellite is still supported (all parameterizations provide the same result at lower energies), its detection in the IACTs regime now looks much more difficult. The total predicted fluxes in γ -rays above 300 GeV and 1 TeV are $\sim 3 \times 10^{-13}$ photons $\text{cm}^{-2} \text{s}^{-1}$ and $\sim 8 \times 10^{-14}$ photons $\text{cm}^{-2} \text{s}^{-1}$, respectively. It can be seen in Figure 6 that Arp 220 is barely below the HESS sensitivity curve (who has to observe Arp 220 at large zenith angle because of its location) and also below MAGIC capabilities unless very deep observations are performed.

7. Concluding remarks

Nearby galaxies, and especially those that are starbursts and luminous infrared galaxies, and thus are subject to a high level of star formation, are prime candidates to constitute a new population of high energy gamma-ray emitters. The definitive observational proof of this statement will most likely come with the launch of GLAST and with further observations of ground Čerenkov telescopes.

Acknowledgments

The work of DFT was performed under the auspices of the U.S. D.O.E. (NNSA), by the University of California Lawrence Livermore National Laboratory under contract No. W-7405-Eng-48. The work of ED-S was done under a FPI grant of the Ministry of Science and Technology of Spain.

^dArp 220 is the nearest ultra-luminous infrared galaxy, in fact it is the only one inside the 100 Mpc sphere, and the best studied.

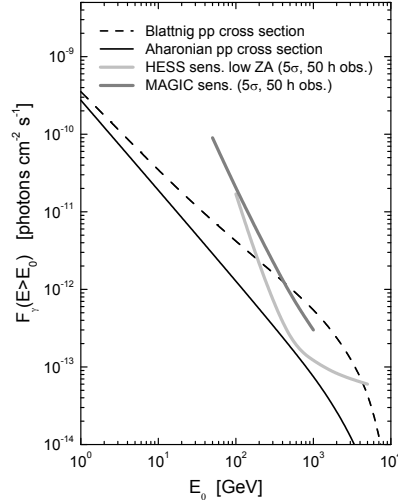


Fig. 6. Total integral flux predictions for Arp 220. The dashed line shows the results obtained with the \mathcal{Q} -DIFFUSE numerical package using Blattnig et al. (2000) parameterization of the pp cross section; the solid line shows the fluxes obtained with the same model but using other cross sections (Aharonian & Atoyan, or Kamae et al.). The HESS and MAGIC telescopes sensitivities, 50 hours of observation time for a 5σ detection, for low zenith angles (although note that this is shown here just for quick comparison, since HESS can only observe Arp 220 above $\sim 50^\circ$), are also shown to remark the differences in predictions for observability that the use of one or other cross section can induce. Absorption effects are already taken into account in both cases.

References

1. Aharonian F. A. & Atoyan, A. M. 1996, *A&A* 309, 91
2. Aharonian F. A. & Atoyan, A. M. 2000, *A&A* 362, 937
3. Aharonian F. A. et al. 2005, *A&A*, in press., [arXiv:astro-ph/0507370]
4. Anchordoqui L. A., et al. 2003b, *ApJ*, 589, 481
5. Anchordoqui L. A. & Torres D. F. 2004, *Rept. Prog. Phys.* 67, 1663
6. Beck R., et al. 1996, *ARAA*, 34, 155
7. Bloemen J. B. G., et al. 1986, *A&A* 154, 25
8. Blom J. J., Paglione T. A. & Carramiñana A. 1999, 516, 744
9. Bradford C. M., et al. 2003, *ApJ* 586, 891
10. Brecher K., Burbidge, G. R. 1972, *ApJ* 174, 253
11. Bronfman L., et al. 1988, *ApJ*, 324, 248
12. Bryant P. M., & Scoville N. Z. 1999, *ApJ* 117, 2632
13. Carilli C. L. 1996, 305, 402
14. Cillis A. N., Torres D. F. & Reimer O. 2005, *ApJ* 621, 139
15. Dame T. M. et al. 2001, *ApJ*, 547, 792
16. Domingo-Santamaría E., & Torres D.F. 2005, *A&A*, in press, [arXiv:astro-ph/0506240]
17. Digel S. W., et al. 2000, [arXiv:astro-ph/0009271]
18. Downes D., & Solomon P.M. 1998, *ApJ* 507, 615

19. Drury L. O'C., Aharonian F. A. & Völk H. J. 1994, A&A 287, 959
20. Engelbracht C. W., et al. 1998, ApJ 505, 639
21. Fichtel C.E., Ozel M.E., Stone R.G. & Sreekumar P. 1991, ApJ, 374, 134
22. Forbes D.A., et al. 1993, ApJ 406, L11
23. Gao, Y., & Solomon, P. M. 2003a, ApJ Suppl. 152, 63
24. Gao, Y., & Solomon, P. M. 2003b, ApJ 606, 271
25. Harrison A., Henkel C. & Russel A. 1999, MNRAS 303, 157
26. Houghton S., et al 1997, A&A 325, 923
27. Hunter, S. D., et al. 1997, ApJ, 481, 205
28. Itoh C., et al. 2002, A&A 396, L1
29. Kamae T., Abe, T. & Koi, T. ApJ, 2005, ApJ 620, 244
30. Lebrun F. et al. 2004, Nature 428, 293
31. Mauersberger R., et al. 1996, A&A 305, 421
32. Melnick J. & Mirabel I. F. 1990, A&A 231, L19
33. Melo V. P., et al. 2002, ApJ 574, 709
34. Özel M.E. & Berkhuijsen E.M. 1987, A&A, 172, 378
35. Pagani L., et al. 1999, A&A 351, 447
36. Pavlidou, V., & Fields, B. 2001, ApJ, 558, 63
37. Rieke G. H., et al. 1980, Ap. J. 238, 24
38. Rieke G. H., Lebofsky M. J. & Walker C. E. 1988, ApJ 325, 679
39. Romero G. E. & Torres D. F. 2003, ApJ 586, L33
40. Sanders, D. B., & Mirabel, I. F. 1996, ARA&A, 34, 749
41. Sanders, D. B., et al. 1998, ApJ 325, 74
42. Solomon P. M., et al. 1987, ApJ 319, 730
43. Solomon, P. M., Downes, D., & Radford, S. J. E. 1992, ApJ, 387, L55
44. Solomon P. M., et al. 1997, ApJ, 478, 144
45. Sorai K., Nakai N., Nishiyama K. & Hasegawa T. 2000, PASJ 52, 785
46. Sreekumar P. et al. 1992, ApJ 400, L67
47. Sreekumar P. et al. 1993, Phys. Rev. Lett., 70, 127
48. Stecker F.W., et al. 1975, ApJ, 201, 90
49. Stephens S. A. & Badhwar G. D. 1981, Astrophysics and Space Science 76, 213
50. Strong, A. W., Moskalenko, I. V., & Reimer, O. 2000, ApJ, 537, 763
51. Torres D. F., et al. 2003, Physics Reports 382, 303
52. Torres D. F. 2004, ApJ 617, 966
53. Torres D. F., Reimer O., Domingo-Santamaría E. & Digel S. 2004, ApJ 607, L99
54. Torres D. F., Domingo-Santamaría E., & Romero G. E. 2004b, ApJ 601, L75
55. Ulvestad J. S. 2000, ApJ 120, 278
56. Ulvestad J. S. & Antonucci R. R. J. 1997, ApJ 488, 621
57. Völk H., Aharonian F. A. & Breitschwerdt D. 1996, Space Science Reviews 75, 279
58. Wild, W., & Eckart A. 2000, A&A 359, 483
59. Young J. S. & Scoville N. Z. 1991, ARA&A 29, 581